J Nanostruct 16(3): 3484-3496, Summer 2026

RESEARCH PAPER

Antibacterial Activity of Green-Synthesized Zinc Oxide Nanoparticles Against Multidrug-Resistant Clinical Pathogens

Sura Qusay Ali [1]*, Hadeel Fayyadh Abbas [2], Farah Abdulkareem [3]

[1] *Department of Biology, College of Education, Aliraqia University, Baghdad, Iraq*

[2] *Department of Laser Science and Technology, Applied Science College, University of Technology, Baghdad, Iraq*

[3] *College of Medicine, Ibn Sina University of Medical and Pharmaceutical sciences, Baghdad, Iraq*

ARTICLE INFO

Article History:
Received 26 March 2026
Accepted 21 May 2026
Published 01 July 2026

Keywords:
Antibacterial activity
Green synthesis
Multi-drug resistance
Pomegranate peel
ZnO nanoparticles

ABSTRACT

Multidrug resistant (MDR) bacteria emergence is a major threat to the worldwide health care and novel antimicrobial agents have been developed. The eco friendly, cost effective and environmentally sustainable synthesis of zinc oxide nanoparticles (ZnO nanoparticles) using pomegranate peel extract (*Punica granatum L.*) as a bio reducing and stabilizing agent is revealed in this study. Ultraviolet-Visible Spectroscopy (UV-Vis), X-ray Diffraction (XRD), Transmission Electron Microscopy (TEM), and Fourier Transform Infrared Spectroscopy (FTIR) were utilized to examine the synthesized ZnO nanoparticles. UV-Vis analysis showed a characteristic absorption peak at 301 nm, and XRD analysis showed a hexagonal wurtzite crystalline structure with an average crystallite size of about 11 nm. TEM imaging showed ultra-fine, quasi spherical primary nanoparticles, mostly in the size range of 4 to 8 nm, belonging to the domain of quantum confinement. FTIR confirmed the presence of organic corona on nanoparticle surface as a result of the existence of pomegranate phytoconstituents such as polyphenols and flavonoids. The antimicrobial activity was performed on clinical multidrug resistant isolates of *Staphylococcus aureus*, *Acinetobacter baumannii* and *Klebsiella pneumoniae* by using agar well diffusion method. Results across all strains showed significant inhibitory effects that were dose dependent. The most sensitive strain was Staphylococcus aureus, which showed 44 mm inhibitory zone at a concentration of 81.38 mg/mL. The zones were somewhat smaller (16-28 mm) due to the complex cell wall structure of Gram-negative bacteria, however, the synthesized ZnO-NPs showed great effectiveness in combating these pathogens. The findings suggest that green-synthesized ZnO nanoparticles are a promising alternative for the treatment of nosocomial infections.

How to cite this article
Ali S., Abbas H., Abdulkareem F. Antibacterial Activity of Green-Synthesized Zinc Oxide Nanoparticles Against Multidrug-Resistant Clinical Pathogens. J Nanostruct, 2026; 16(3):3484-3496. DOI: 10.22052/JNS.2026.03.040

INTRODUCTION

Bacterial diseases provide a significant concern for human health, having been the second leading cause of death as of 2019 [1]. In recent years, a primary worry associated with microbial illnesses is drug resistance. The World Health Organization asserted that, consequently, infections have become more challenging to treat [2]. Since the advent of antibiotics in the 20th century, bacteria have developed by acquiring defensive mechanisms that diminish or eliminate antibiotic efficacy [3,4]. Currently, pharmaceutical

* *Corresponding Author Email: sorra.q.ali@aliraqia.edu.iq*

corporations are diminishing their interest in the study of novel antibiotics due to elevated expenses and the protracted period of studies, coupled with uncertain financial and therapeutic outcomes [5]. To solve antibiotic resistance, the WHO established a list of priority infections necessitating the development of novel antimicrobials [6]. It encompasses 'ESKAPE' pathogens, including *Enterococcus faecium, Staphylococcus aureus, Klebsiella pneumoniae, Acinetobacter baumannii, Pseudomonas aeruginosa,* and *Enterobacter spp.* The majority are multidrug-resistant isolates, presenting a significant difficulty in clinical practice. It markedly prolongs hospital duration, elevates care expenses, and heightens fatality rates. Furthermore, ESKAPE pathogens are the predominant cause of nosocomial infections globally [7].

Drug resistance results from several complex mechanisms, including increased efflux pump expression, which removes medications from the bacterial cell; genes that change the binding substrate, which changes drug targets; and proteins and enzymes that alter pharmaceuticals [8]. Multidrug-resistant organisms include *E. coli, S. aureus, and P. aeruginosa* [9]. Bacteria build biofilms to resist antibiotics [10]. A "structured community of bacterial cells enclosed in a self-produced polymeric matrix and adherent to an inert or living surface" is a bacterium biofilm, which helps bacteria survive in hostile settings [11]. They exchange nutrients via channels and express various genes in various regions of biofilm [12]. Biofilm spatial heterogeneity permits some of the biofilm to withstand antibiotic attack, thereby causing antibacterial resistance [11,13,14]. Antimicrobials diffuse slower in biofilms than in water [11,15], allowing bacteria biofilms to tolerate antibiotic concentrations up to 1000 times higher than planktonic bacteria [16]. Therefore, it is imperative to explore novel therapeutic strategies for the treatment of infections induced by ESKAPE pathogens. Currently, multidrug resistance (MDR) constitutes the primary obstacle in the development of antibacterial drugs, posing a significant risk to human health and presenting a substantial concern for healthcare system expenditures [15]. Accordingly, there is an immediate necessity to identify alternative approaches that can effectively address bacterial infections, with nanomaterials being potential options for antibacterial efficacy [17].

Nanotechnology encompasses the creation and manipulation of nano-scale information inside a restricted area of materials, devices, and measurements. Materials at the nanoscale are engineered into discrete units termed nanoparticles (NPs), which consist of atoms and molecules measuring between 1 and 100 nm in size. It is widely utilised to create more efficient approaches in technology, energy conservation, scientific research, medicine, and various other domains. Nanoscale particles are produced using several methodologies, encompassing biological, chemical, and physical techniques. These methods are categorised as bottom-up and top-down approaches [18]. Biological or green synthesis is a bottom-up process that uses natural and ecologically acceptable reducing agents. Sometimes green materials are utilised as end-capping agents and dispersants [19]. Green nanoparticle synthesis is simple to solve cost-effective, and eco-friendly. However, green synthesis strategies for nanoparticles may improve their properties due to their smaller dimensions, particular form, and unique biological substrates [20].

Zinc oxide nanoparticles (ZnO-NPs) are metal oxide nanomaterials with unique physical and chemical characteristics. These inorganic chemicals have many everyday uses. ZnO-NPs are the most widely used metal oxide nanoparticles because their optical and chemical properties can be easily adjusted by changing their morphology, wide bandgap, and high excitation binding energy, making them potent photocatalytic and photo-oxidizing moiety against biological and chemical species [21]. They demonstrate less toxicity to the human body and ensure biocompatibility, as the Zn ion (Zn^{+2}), a soluble variant of ZnO, is a trace element found in the human physiological system. ZnO has exhibited biodegradable in both its bulk form and as nanoparticle [22]. One of the most therapeutic plants is pomegranate (Punica granatum L.). In the Punicaceae family, its common name comes from the Latin words ponus and granatus, meaning "seeded apple." This wonderful fruit, from Afghanistan, Iran, China, and India, is eaten globally [23]. Fruit structure demonstrates its medicinal properties. The internal membrane network of pomegranate peels (PoP) accounts for 26–30% of the fruit weight. Phenolic chemicals such anthocyanins, catechins, and hydrolysable tannins like punicalin, pedunculagin, punicalagins,

gallic, and ellagic acid are abundant in these peels. Their concentration in the peel and juice accounts for 92% of the fruit's antioxidant action, according to research [24]. Also, Gallic acid, ellagic acid, and punicalagin are powerful antibacterials and free radical scavengers.

They are particularly effective against enteric infections such *E. coli, Salmonella, Shigella*, and *Vibrio cholerae* [25]. Pomegranate peel extract (PoPx) has been used therapeutically for ages in many cultures. Egyptians used it to cure inflammation, diarrhoea, intestinal parasites and respiratory difficulties.

This old wisdom has prompted rigorous modern scientific studies into human health. The active compounds in pomegranate extracts prevent and treat gastro mucosal injuries, cancer chemoprevention and diabetes related oxidative damage according to recent studies [26]. The antibacterial effect of PoP phenolics is based on mechanistic evidence that shows how lysis of microbial cells occurs through the precipitation of membrane proteins. Without further enrichment from other fruit sections, the peel's high phytochemical concentration makes it a useful traditional and scientific asset [27]. When used in nanoparticle manufacturing, the bioactive components of pomegranate peels help stabilise and reduce the size of the final product.

The resulting ZnO-NPs can have improved optical characteristics, size, and shape when these chemicals are added. Metallic nanoparticles have gained recognition for their substantial antibacterial efficiency against human illnesses [28], and nanotechnology offers good solutions across a variety of applications. Therefore, ZnO-NPs' antibacterial activity has garnered a lot of attention because of their unique bactericidal processes, which include their capacity to interact with bacterial surfaces and penetrate the bacterial core, where they enter the cell [29]. The biological benefits of pomegranate peel can be harnessed using ZnO-NPs synthesised using this fruit's extract. The inherent antibacterial characteristic of zinc gives the ZnO-NPs improved antibacterial and antimicrobial capabilities.

The objectives of this study were: to synthesize ZnO nanoparticles via a green, cost-effective route using pomegranate peel extract as a reducing and stabilizing agent and characterize it using different methods, and to evaluate their antibacterial efficacy against multidrug-resistant clinical isolates.

MATERIALS AND METHODS

Chemicals and Instruments

All chemicals employed in the synthesis and analytical methods were rated as analytical reagent (AR) quality and utilised without additional purification except if specified differently. Zinc nitrate hexahydrate [$Zn(NO_3)_2{\cdot}6H_2O$; CAS No. 10196-18-6; M.Wt. = 297.49 g/mol; catalogue No. 695595; minimum assay ≥99.0% (complexometric); pH of 10% aqueous solution: 3–6; CDH Fine Chemicals, Delhi, India] was utilized as the zinc precursor for nanoparticle manufacturing. The chemical is characterized as colorless or white crystals, readily soluble in water, producing a clear, colorless solution. Deionized water was utilized as the solvent in all preparatory stages. Ethanol (Duksan, Korea) was utilized for the washing and purifying of the resulting nanoparticle precipitate. Mueller–Hinton agar (Accumix/Oxoid, UK) served as the culture media for bacterial antimicrobial

Table 1. Chemicals utilized in the study.

No.	Chemical	Specification	Manufacturer	Country
1	Zinc Nitrate Hexahydrate $Zn(NO_3)_2{\cdot}6H_2O$ CAS: 10196-18-6 M.Wt: 297.49 g/mol Cat. No. 695595	AR grade, ≥99.0% 500 g pH (10%): 3–6	CDH Fine Chemicals	India
2	Ethanol (C_2H_5OH)	AR grade	Duksan	Korea
3	Mueller–Hinton Agar	Dehydrated powder	Accumix/Oxoid	UK
4	Distilled Water (DIW)	In-house distillation	—	—
5	Normal Saline (0.9% NaCl)	Sterile	—	—

tests. The whole list of instruments and the requirements specified are presented in Tables 1 and 2.

Preparation of Pomegranate Peel Extract

Fresh pomegranates fruits (Punica granatum L.) were obtained from a nearby commercial supplier. After physically removing the peels from the fruit, they were washed with distilled water to remove any surface impurities. After that they were dried in a convection oven at 60°C until they reached a stable weight. Afterwards, a laboratory grinder was used to ground the dried peels into a fine powder.

For the extraction process, ten grams of dried peel powder were added to a 250 mL Erlenmeyer flask that already contained 200 mL of distilled water. Phytoconstituent extraction was ensured by subjecting the mixture to a hot-plate magnetic stirrer and heating it to 80°C while stirring constantly for 15 minutes. The conical-shaped Whatman No. 1 filter paper was used to filter the resulting dark orange-brown suspension. A glass funnel was placed in the funnel and held in place on a retort stand with a metal clamp. A 250 mL glass beaker was used to collect the filtrate.

The clear, pale yellow to light greenish filtrate showed that insoluble peel residue was removed. To clarify the extract and remove microscopic particles, the filtrate was centrifuged at 1500 r/min. The refined pomegranate peel extract was stored at 5°C until nanoparticle production.

Green Synthesis of ZnO Nanoparticles

A 1 M stock solution of zinc nitrate hexahydrate [$Zn(NO_3)_2 \cdot 6H_2O$/ CDH Fine Chemicals, India/ CAS No. 10196-18-6; Molecular Weight = 297.49 g/mol; purity ≥99.0% AR] was formulated by dissolving

Table 2. Instruments and equipment utilized in the study.

No.	Instrument / Equipment	Manufacturer	Country
1	Hot plate magnetic stirrer	Four E's	China
2	Analytical balance (4-digit)	Hangzhou / Kern pfb	China / Germany
3	Erlenmeyer flask (glass)	Pyrex	Germany
4	Round-bottom flask	Labmax	Germany
5	Autoclave	Westlne / Faithful	China
6	Laminar flow cabinet	Faithful	China
7	Incubator	Ningbo / Faithful	China
8	Centrifuge	—	—
9	UV–Vis spectrophotometer	—	—
10	Distillator	GFL	Germany
11	Densichek (turbidity meter)	bioMérieux	France
12	Micropipette (10–100 µL)	Biopette	Germany
13	Wooden inoculation sticks	Biozek	Netherlands
14	Glass beaker (600 mL / 250 mL)	Simax	Czech Republic
15	Glass funnel (filtration)	—	—

59.49 g of the salt, calculated using the formula: wt = M × M.Wt × V = 1 mol/L × 297.49 g/mol × 0.200 L, in 200 mL of distilled water. The solution was transferred to a flask and magnetically stirred for 15 minutes at ambient temperature to complete dissolution, yielding a clear, colorless solution that matches the molecule's solubility profile.

Pomegranate peel extract was slowly added to zinc nitrate while magnetically swirling to synthesize nanoparticles. The extract worked as both a bio-reducing and surface-capping agent, transforming Zn^{+} ions into Zinc Oxide nuclei. A color change indicated nanoparticle formation after constant agitation. Allowing the reaction to finish.

Ultra Violet visible spectroscopy investigation

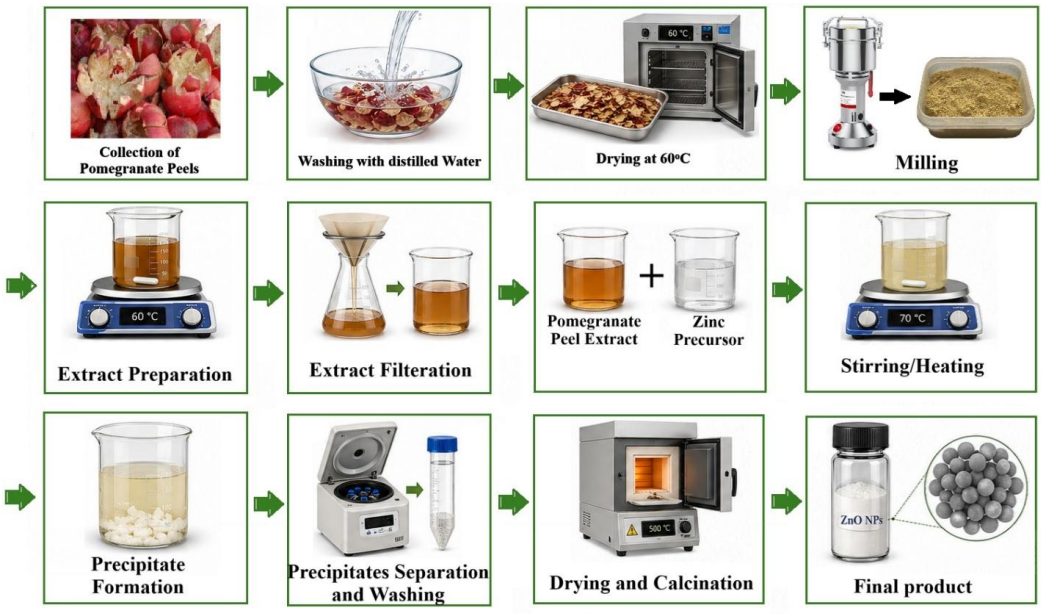

(a)

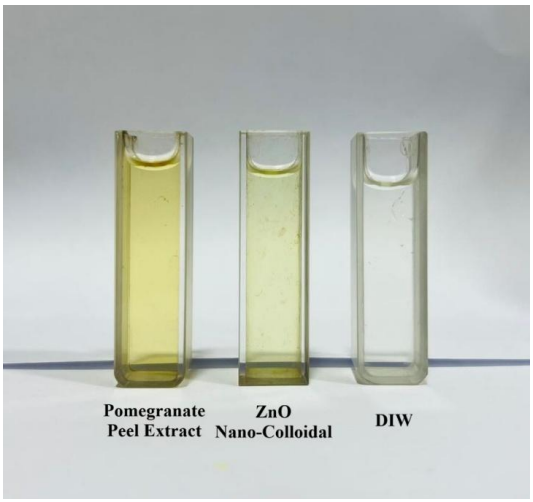

(b)

Fig. 1. (a) Schematic representation of experimental procedure for the green synthesis of ZnO nanoparticles using pomegranate peel extract, (b) ZnO Nano-colloidal.

confirmed the generation of Zinc Oxide nanoparticles by showing a unique absorption peak at 301 nm for the synthesized Zinc Oxide Nanoparticles solution, compared to 374 nm for the pomegranate peel extract. The blue shift concerning the extracted peak and the deviation from the bulk ZnO band edge (~380 nm) validated the development of nanoscale ZnO. The theoretical maximum concentration of ZnO in the final solution was determined under the assumption of complete conversion of Zn^{+2} to ZnO:

L × 81.38 g/mol = 16.276 g. ZnO concentration = 16.276 g / 0.200 L = 81.38 g/L = 81.38 mg/mL (100% stock, Sample E).

moles = C × V = 1 mol/L × 0.200 L = 0.200 mol ZnO
mass = moles × M.Wt = 0.200 × 81.38 = 16.276 g

After nanoparticle synthesis, the suspension underwent centrifugation to precipitate the nanoparticles and eliminate unreacted precursors and residual organic contaminants. The particle was progressively washed with distilled water and ethanol, then resuspended in distilled water to produce a purified ZnO-NP stock suspension at a theoretical concentration of 81.38 mg/mL. Serial dilutions of the stock solution (50%, 25%, and 12.5%) were produced in distilled water immediately before antibacterial examination (Table 3).

Bacterial Isolates and Culture Conditions

Multidrug-resistant (MDR) clinical isolates of *Staphylococcus aureus* (Gram-positive), *Acinetobacter baumannii* (Gram-negative), and *Klebsiella pneumoniae* (Gram-negative) were procured from Microbiology Laboratory of Ibn Al-Quff Hospital, Baghdad, Iraq. The multidrug-resistant (MDR) phenotype of each isolate was validated using conventional antimicrobial susceptibility testing utilizing the modified Kirby–Bauer disc diffusion method in accordance with the Clinical and Laboratory Standards Institute recommendations [30]. Stock cultures were preserved on nutrient agar slopes at 4°C and subcultured onto suitable media before each of the experiments.

Preparation of Culture Media

Mueller–Hinton agar (MHA; Oxoid, UK) was formulated according to the manufacturer's guidelines. 38 grams of the dried powder were dissolved in one liter of distilled water. The suspension was heated with constant agitation on a hob until the powder was all dissolved. The medium was then sterilized using autoclaving at 121°C for 15 minutes. After autoclaving, the medium was permitted to cool to roughly 50°C in a water bath, after which approximately 20 mL was aseptically transferred onto sterile 90 mm polystyrene Petri plates. Plates were positioned on a flat surface for about 15 minutes to facilitate solidification, thereafter, inverted and stored at 4°C until required.

Antibacterial Activity Assay

The inoculum was made from overnight nutrient agar cultures of all bacterial isolates. Inoculated morphologically symmetrical colonies into 3 mL of sterile normal saline via a sterile wire loop. Turbidity was measured to 0.5 McFarland standard (1*108 CFU/mL) using a Densichek turbidity meter (bioMerieux, France). The inoculum sued within

Table 3. ZnO NPs test concentrations used in the antibacterial assay.

Sample Label	Dilution	Concentration (mg/mL)	Description
A	Negative control	0	Distilled water (DIW)
B	12.5%	10.17	1:8 dilution of stock
C	25%	20.35	1:4 dilution of stock
D	50%	40.69	1:2 dilution of stock
E	100%	81.38	Undiluted stock

15 minutes of manufacture.

Zinc Oxide Nanoparticles samples were tested for antibacterial activity using the modified agar well-diffusion method [30]. After cooling, 20 mL of molten MHA was poured into sterile Petri dishes to solidify. A sterile brush was immersed in the usual bacterial mixture and pressed against the tube wall to remove excess fluid to infect each plate. To ensure even coverage the swab was spread throughout the agar surface in three directions and turned 60° after each application. The swab was then put to the agar's inner perimeter. To desiccate inoculated plates they were kept at room temperature for three minutes with closed lids.

With a sterile bio pette tip, 6 mm wells were formed in the agar. Each well was carefully filled with 50 microliters of Zinc Oxide Nanoparticles (Samples B, C, D, or E) or distilled water (Sample A (negative control)). In aerobic conditions plates incubated at 37°C for 18 to 24 hours. Incubation was followed by millimeter measurements of the zone of inhibition (ZOI) surrounding each well with a calibrated ruler.

Following recognized breakpoints, the modified Kirby Bauer disc diffusion method [30] was used to assess the isolates antibiotic susceptibility [31]. As previously described MHA plates were infected with 0.5McFarland bacterial suspensions.

Commercial antibiotic discs were placed on the inoculated agar surface using sterile forceps, pushed lightly to ensure total contact and incubated at 37°C for 18 to 24 hours.ZOI were measured and classed as sensitive, moderate or resistant [31]. Only MDR isolates were tested for ZO Nanoparticles.

RESULTS AND DISCUSSION

UV visible Spectroscopy

The absorption spectra of the synthesized ZnO sample had an absorption peak at 301 nm, while the pomegranate peel extract had a peak at 373 nm. This suggests that the electronic environment underwent a substantial change after interacting with zinc ions and forming a new nanophase. The blue shift can be ascribed to the reduced nanoscale dimensions the increased ratio of surface atoms and the influence of plantderived compounds on the particle surface. The absorption peak at 301 nm is markedly blueshifted relative to both the pomegranate peel extract and the approximately 380 nm band edge of bulk ZnO signifying a hypochromic shift associated with nanoscale size reduction. As particle dimensions decrease quantum confinement raises the effective band gap and shifts the absorption start to shorter wavelengths. Thus the optical response supports the idea that the synthesized ZnO was nanoscale.

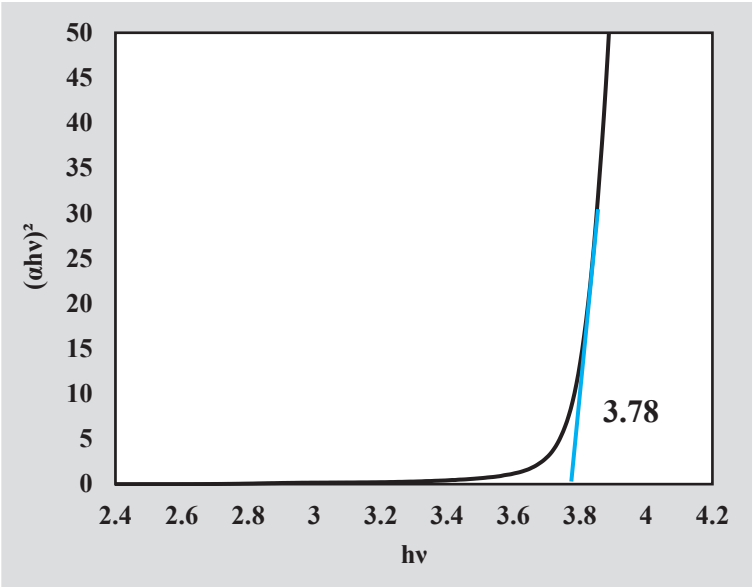

Fig. 2. The Tauc plot ((αhv) ² against (hv)) of green synthesized Zinc Oxide Nanoparticles indicates an estimated optical band gap energy of Eg = 3.78 eV.

The 301 nm peak shows that the organic surface layer didn't merely encapsulate ZnO but actively limited particle development during nucleation and stabilization [32-34].

The optical band gap from the Tauc plot (Eg=3.78 eV) confirms this perspective, as it greatly exceeds bulk ZnO, confirming the nanoscale band gap increase (Fig. 2). The TEM-derived particle size range of 4 to 8 nm implies that synthesized ZnO nanoparticles have a broader band gap aligning with quantum-confined nanostructure dimensions and optical properties rather than bulk like ZnO [34].

X-Ray Diffraction (XRD)

The diffraction peaks showed peaks at 2θ = 31.77°, 34.42°, 36.25°, 47.54°, 56.60°, 62.86°, 66.38°, 67.96°, 69.10°, 72.56°, and 76.95° were assigned to the (100), (002), (101), (102), (110), (103), (200), (112), (201), (004), and (202) planes of hexagonal wurtzite ZnO, aligning well with standard JCPDS/PDF card No. 36-1451 [35, 36].

Conversely specific XRD peaks at about 31.6, 34.3 and 36.0 among others indicate the hexagonal wurtzite structure of ZnO showing that the synthesized substance is nanocrystalline zinc oxide and an organometallic complex.

The product's phase purity and crystallinity were verified by XRD. The absence of extraneous diffraction peaks rules out phase contamination by zinc hydroxide or unreacted precursor, confirming that the product is phase pure crystalline ZnO[37].

The Debye Scherrer equation was used to calculate the average crystallite size of synthesized ZnOnanoparticles from XRD peaks [38]. The analyzed reflections had crystallite sizes ranging from 4.6 to 27.4 nm, with an average of 11 nm.

This value matches the nanoscale domain, giving independent diffraction-based confirmation that the synthesized material comprises crystalline ZnO domains restricted to the lower nanoscale range. The comparatively wide FWHM values noted in most reflections smaller coherent scattering domains increase peak broadening in accordance with the Scherrer equation, as shown for green synthesized ZnO nanoparticles of similar dimensions derived from polyphenol rich plant extracts.

According to the literature plant derived ZnO has an absorption edge in the UV spectrum due to its crystalline wurtzite structure and aggregated spherical or quasi spherical shape. This work found similar patterns [39].

Transmission Electron Microscopy (TEM) and Particle Size Distribution

Transmission Electron Microscopy images as in Fig. 3, showed that the green synthesized zinc oxide from pomegranate peel extract contains ultrafine nanoparticles with dimensions near the quantum-confinement regime, quasi spherical to irregular quasispheroidal shapes, and a propensity for secondary agglomeration. At 100 nm low magnification photos show condensed nano agglomerations in an inhomogeneous arrangement but at 20 and 10 nm these agglomerations are made of much smaller primary units packed tightly within nanoclusters.

Particle size spans from 4 to 8 nm with significant concentration at 5 ± 2 nm. Quantitative size analysis using TEM micrographs showed a mean diameter of 4.09±1.88 nm and a median of 2.98 nm with many particles in the 2 to 4 nm range and most of the material in the 2 to 8 nm range, indicating that the synthesized nanoparticles are in the quantum confinement domain of ZnO.

Pomegranate peel phytoconstituents excellent surface passivation during nucleation stops crystal growth early and promotes a very small primary particle population as shown by the right skewed distribution profile. Green route ZnO synthesis often uses plant based reducing agents and has a two tiered design with discrete ultrasmall primary units merged into loose secondary clusters. This morphological style is characterized by green ZnO synthesis which has a high surface energy and dipole nature.

The remaining plant derived compounds on the surface form tiny primary units that form secondary clusters. The tendency for secondary agglomeration is due to ZnO high surface energy and polar wurtzite lattice, which encourage particle particle attraction after nucleation.

Similar structures have been seen in green synthesized ZnO using Punica granatum extract with various degrees of aggregation. However, the study particles are smaller and more densely aggregated [40].

The mean diameter from direct TEM measurements matches crystallite sizes from Debye Scherrer analysis of XRD peak broadening independently validating that TEM micrographs show coherent crystalline domains. Keeping those clusters extremely small primary units preserves

the material's biologically functional high surface to volume ratio.

Fourier Transform Infrared Spectroscopy

It was confirmed FTIR results morphological interpretation with broad bands in the 3248-3498 cm^{-1} range indicating hydroxyl groups, likely polyphenols and tannins in pomegranate peel.

Conversely, the bands at 1622-1741 cm^{-1} align with plant extract carbonyl groups and organic chemicals, as well as flavonoids and organic acids maintained on the nanoparticle surface post synthesis, bonds between carbon and oxygen in the bands at 1141 and 1006 cm^{-1} support the organic coating idea, whereas the peculiar band at 451 cm^{-1} confirms zincand oxygen bonding and lattice vibration [41, 42].

Thus, TEM provides direct morphological evidence that supports the structural findings from XRD, the optical results from UV, and the chemical analysis from FTIR validating the green production of ZnO nanoparticles using pomegranate peel extract. The convergence analysis of XRD, TEM, UV visible, and FTIR validates the green manufacture of crystalline ZnO nanoparticles with pomegranate derived phytoconstituents.

Structure–Activity Relationship

Research shows that phenolic and organic compounds in pomegranate peel extract not only reduced synthesis but also partially coated and stabilized nanoparticle surfaces creating a durable organic corona close closeness of tiny particles.

Transmission Electron Microscopy images show that surface organic molecules reduce crystal growth and sterically inhibit crystallite coalescence, while ZnO's high surface energy and polarity drive secondary agglomeration. The data of FTIR show that ZnO was successfully synthesized and that nanoparticles in TEM micrographs are ultrafine primary units grouped into nanoclusters a hallmark of green synthesized nanomaterials.

This organic corona may increase nanoparticle dispersibility in aqueous biological settings and electrostatic interactions with bacterial cell membranes, contributing to their antibacterial activity [41].

The antibacterial activity of synthesized ZnO is closely related to this nanostructure. The smaller primary particle size and increased specific surface area promote direct interaction with the bacterial cell.

They stimulate Zn^{+2} ions release and the formation of reactive oxygen species (ROS), which are critical mechanisms that affect permeability of the membrane induce oxidative stress and impede metabolic processes in bacterial cells.

Similarly, the presence of permanent surface organic groups, as demonstrated byFTIR, may enhance the stability of nanoparticles, and improve their interaction with the biological milieu.

The formation of ultra fine ZnO particles aggregated into nanoclusters, as depicted in TEM micrographs, should not be viewed as a structural flaw, but rather as a deliberate morphological configuration conducive to enhanced biological efficacy against clinically significant multidrug-resistant pathogens.

Thus, TEM, UV visible, FTIR and XRD results strongly suggest that pomegranate peel extract

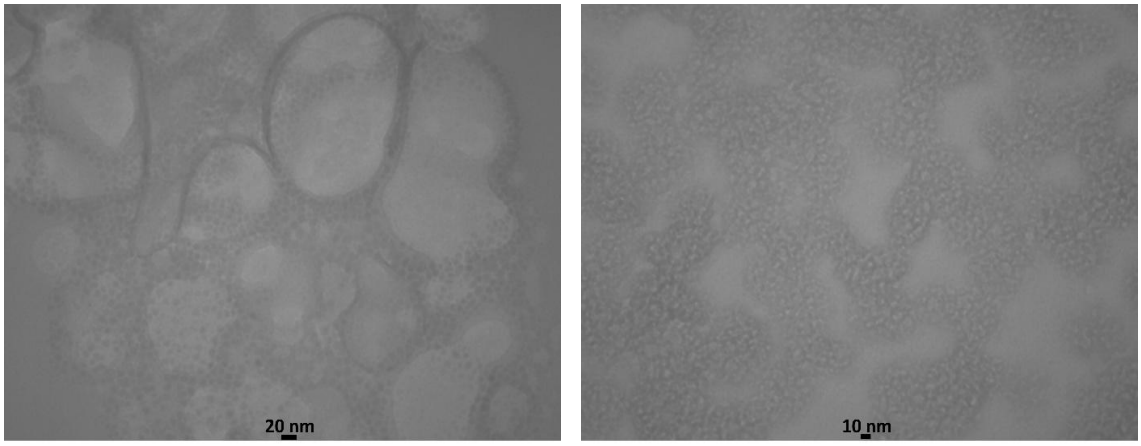

Fig. 3. Transmission electron microscopy (TEM) micrographs of green synthesized ZnO nanoparticles at 20 nm and 10 nm scale bars.

reduced and stabilized nanoparticles and formed bioactive and crystalline small sized nano ZnO making it an attractive option for hospital infection prevention [43,44].

Antibacterial activity of ZnO-NPs

All three trials show a dose dependent relationship. From 12.5% (B) to 100% (E), ZnO nanoparticle concentration increases the Zone of Inhibition (ZOI). Sample A (Control) shows little to no inhibition demonstrating that distilled water is not antibacterial and that the nanoparticles are the only factor. Sample E (100%) consistently has the maximum ZOI indicating excellent efficacy at maximal concentration.

The nanoparticles eliminate Gram-positive *S. aureus* and Gram-negative *A. baumannii, K. pneumoniae* bacteria, but sensitivity varies. At 100% concentration (81.38 mg/ml), *S. aureus* showed a 44 mm inhibitory zone bigger than the others. Even at low doses 12.5% maintained a 30 mm zone of inhibition.

A. baumannii displays slightly higher sensitivity than *K. pneumoniae*, reaching approximately 28 mm at 100% concentration. As illustrated in Figs. 4-6, *K. pneumoniae* displays ZOI ranging from approximately 16 mm (12.5%) to 24 mm (100%).

The study found that ZnO nanoparticles concentrations enhance the ZOI. *S. aureus* is highly susceptible to green-synthesized ZnO nanoparticles. Gram positive bacteria lack the outer lipopolysaccharide (LPS) membrane of Gram negative bacteria, making them more susceptible to nanoparticle invasion. These strains are notoriously multi drug resistant. Gram positive bacteria lack an exterior protective barrier but have a strong, permeable peptidoglycan layer.

This arrangement improves ZnO nanoparticle cell penetration. Premanathan *et al.* (2011) found that Gram positive bacteria are more susceptible to ZnO nanoparticles due to their negative cell walls, which attract positively charged Zn^{2+} ions and cause membrane damage. The fact that ZnO nanoparticles have different zones beyond 20 mm suggests they can fight these robust illnesses [45].

baumannii and K. pneumoniae have smaller inhibitory zones (16 to 28 mm). Gram negative bacteria have greater resistance to the LPS membrane, according to the literature. Nanoparticles can't enter the cytoplasm through this membrane's chemical barrier. *A. baumannii* is resistant to traditional antibiotics, however metal

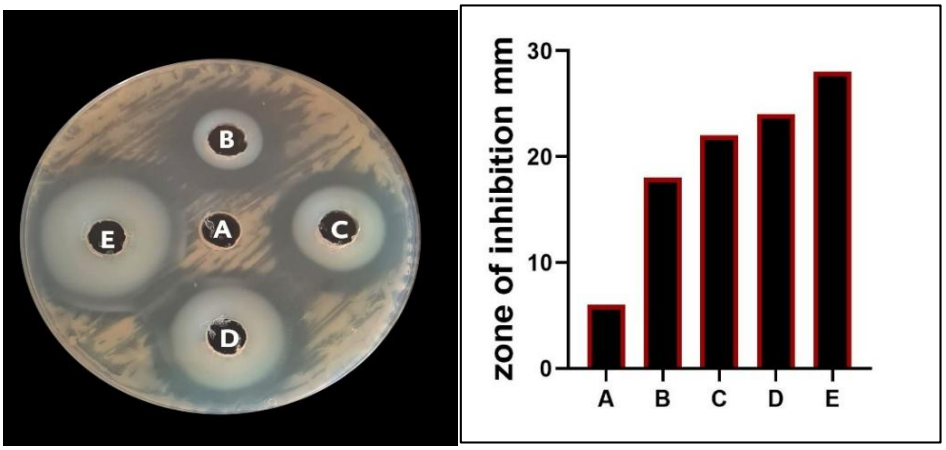

Fig. 4. Antibacterial activity of ZnO NPs against *A. baumannii.* A, Control (DIW). B, 12.5 %. C, 25 %. D, 50 %. E, 100 %.

Table 4. Antibacterial activity of ZnO nanoparticles against MDR bacteria.

Strain	12.5% (B)	25% (C)	50% (D)	100% (E)
S. aureus	30 mm	35 mm	40 mm	44 mm
A. baumannii	~18 mm	~22 mm	~24 mm	~28 mm
K. pneumoniae	~16 mm	~18 mm	~22 mm	~24 mm

oxide nanoparticles can physically break the cell membrane and bypass resistance mechanisms like efflux pumps [46].

Many Klebsiella bacteria create a capsular polysaccharide that "trap" nanoparticles and impede their passage to the cell membrane, which may explain *K. pneumoniae* lower sensitivity this physical entrapment process adds resistance beyond the outer membrane barrier and may explain the decreased ZOI levels compared to other strains. This matches the results correspond with the observations of Rizwan *et al.* (2010), and Alekish *et al.* (2025), who found that high nanoparticle concentrations increase reactive oxygen species (ROS), which damage bacterial DNA and proteins or disrupt cell walls by aggregating

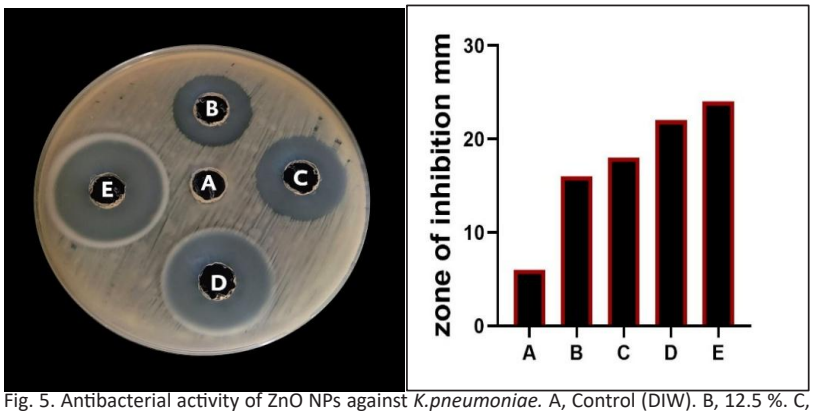

Fig. 5. Antibacterial activity of ZnO NPs against *K.pneumoniae.* A, Control (DIW). B, 12.5 %. C, 25 %. D, 50 %. E, 100 %.

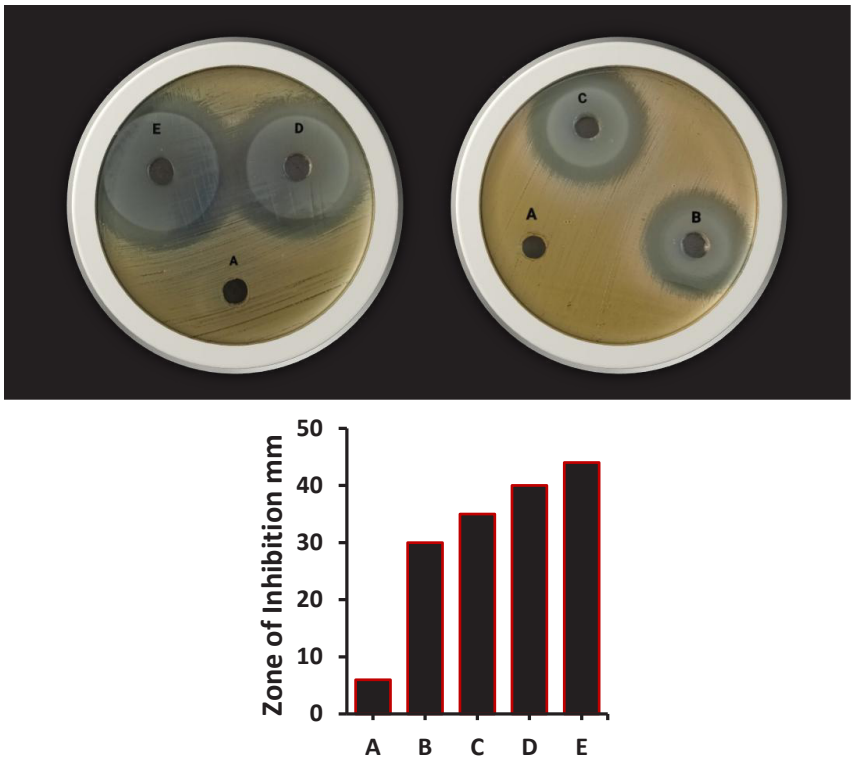

Fig. 6. Antibacterial efficacy of ZnO NPs against Methicillin Resistant *S.aureus.* A, Control (DIW). B (12.5%), C (25%), D (50%), E (100%).

on the bacterial surface and "pitting" the cell wall [47, 48]. Alternatively, Zn^{+2} ions may enter the cell and disturb metabolism. Nanoparticle cell wall interactions grow with concentration, causing oxidative stress and cell death.

The phytochemical components of the pomegranate peel extract preserved on the nanoparticle surface by FTIR, are known to have antibacterial activities and may improve the zinc oxide core's inhibitory effectiveness. This synergistic method may enhance the antibacterial activity of nanoparticles containing plant bioactive compounds such as flavonoids and polyphenols compared to chemically synthesized ZnO [32].

CONCLUSION

In this study, bioactive ZnO NPs were synthesized by eco friendly approach using pomegranate peel extract. Detailed characterization confirmed the presence of crystalline ultra fine nanoparticles ~4-8 nm that stabilized by organic layer of phytochemicals derivedfrom plants. The synthesized ZnO NPs showed a marked dose dependent antibacterial activity against clinically relevant MDR pathogens; *S. aureus, A. baumannii,* and *K. pneumoniae*. Bacterial cell wall composition affects activity of NPs as indicated by higher sensitivity of Gram positive *S. aureus* strains as compared to Gram negative strains. The organic corona made from pomegranates and the zinc oxide core synergistically improve the biological performance of nanostructures, which enhance the intrinsic antibacterial properties of the core to resist antibiotic resistance and address the urgent need for new therapies in clinical applications. The results indicate that ZnO nanoparticles synthesized by green synthesis are an effective, practical and environment friendly solution.

CONFLICT OF INTEREST

The authors declare that there is no conflict of interests regarding the publication of this manuscript.

REFERENCES

1. Global, regional, and national burden of 12 mental disorders in 204 countries and territories, 1990–2019: a systematic analysis for the Global Burden of Disease Study 2019. The Lancet Psychiatry. 2022;9(2):137-150.
2. Klein EY. Antibiotic Resistance. Oxford Medicine Online: Oxford University Press; 2016.
3. Cohen ML. Changing patterns of infectious disease. Nature. 2000;406(6797):762-767.
4. Yeaman MR, Yount NY. Mechanisms of Antimicrobial Peptide Action and Resistance. Pharmacol Rev. 2003;55(1):27-55.
5. Szul M. Causes Behind the Global Crisis of Increasing Antibiotic Resistance and Strategies to stop this. Polygence; 2024. http://dx.doi.org/10.58445/rars.1194
6. Global antibiotic resistance surveillance report 2025: World Health Organization; 2025 2025/10/13.
7. Marturano JE, Lowery TJ. ESKAPE Pathogens in Bloodstream Infections Are Associated With Higher Cost and Mortality but Can Be Predicted Using Diagnoses Upon Admission. Open Forum Infectious Diseases. 2019;6(12).
8. Khan SN, Khan AU. Breaking the Spell: Combating Multidrug Resistant 'Superbugs'. Front Microbiol. 2016;7.
9. Alekshun MN, Levy SB. Molecular Mechanisms of Antibacterial Multidrug Resistance. Cell. 2007;128(6):1037-1050.
10. Huh AJ, Kwon YJ. "Nanoantibiotics": A new paradigm for treating infectious diseases using nanomaterials in the antibiotics resistant era. Journal of Controlled Release. 2011;156(2):128-145.
11. Costerton JW, Stewart PS, Greenberg EP. Bacterial Biofilms: A Common Cause of Persistent Infections. Science. 1999;284(5418):1318-1322.
12. Davies DG, Chakrabarty AM, Geesey GG. Exopolysaccharide production in biofilms: substratum activation of alginate gene expression by Pseudomonas aeruginosa. Applied and Environmental Microbiology. 1993;59(4):1181-1186.
13. Huang C-T, Xu KD, McFeters GA, Stewart PS. Spatial Patterns of Alkaline Phosphatase Expression within Bacterial Colonies and Biofilms in Response to Phosphate Starvation. Applied and Environmental Microbiology. 1998;64(4):1526-1531.
14. Xu KD, Stewart PS, Xia F, Huang C-T, McFeters GA. Spatial Physiological Heterogeneity in Pseudomonas aeruginosa Biofilm Is Determined by Oxygen Availability. Applied and Environmental Microbiology. 1998;64(10):4035-4039.
15. Stewart PS. Diffusion in Biofilms. J Bacteriol. 2003;185(5):1485-1491.
16. Gebreyohannes G, Nyerere A, Bii C, Sbhatu DB. Challenges of intervention, treatment, and antibiotic resistance of biofilm-forming microorganisms. Heliyon. 2019;5(8):e02192.
17. Zheng K, Setyawati MI, Leong DT, Xie J. Antimicrobial silver nanomaterials. Coord Chem Rev. 2018;357:1-17.
18. Joudeh N, Linke D. Nanoparticle classification, physicochemical properties, characterization, and applications: a comprehensive review for biologists. Journal of Nanobiotechnology. 2022;20(1).
19. Banjara RA, Kumar A, Aneshwari RK, Satnami ML, Sinha SK. A comparative analysis of chemical vs green synthesis of nanoparticles and their various applications. Environmental Nanotechnology, Monitoring and Management. 2024;22:100988.
20. Ijaz I, Gilani E, Nazir A, Bukhari A. Detail review on chemical, physical and green synthesis, classification, characterizations and applications of nanoparticles. Green Chemistry Letters and Reviews. 2020;13(3):223-245.
21. Shaba EY, Jacob JO, Tijani JO, Suleiman MAT. A critical review of synthesis parameters affecting the properties of zinc oxide nanoparticle and its application in wastewater treatment. Applied Water Science. 2021;11(2).
22. Mandal AK, Katuwal S, Tettey F, Gupta A, Bhattarai S, Jaisi S, et al. Current Research on Zinc Oxide Nanoparticles: Synthesis, Characterization, and Biomedical Applications. Nanomaterials. 2022;12(17):3066.
23. Patel C, Dadhaniya P, Hingorani L, Soni MG. Safety

assessment of pomegranate fruit extract: Acute and subchronic toxicity studies. Food and Chemical Toxicology. 2008;46(8):2728-2735.
24. Afaq F, Saleem M, Krueger CG, Reed JD, Mukhtar H. Anthocyanin- and hydrolyzable tannin-rich pomegranate fruit extract modulates MAPK and NF-κB pathways and inhibits skin tumorigenesis in CD-1 mice. Int J Cancer. 2004;113(3):423-433.
25. Bachoual R, Talmoudi W, Boussetta T, Braut F, El-Benna J. An aqueous pomegranate peel extract inhibits neutrophil myeloperoxidase in vitro and attenuates lung inflammation in mice. Food and Chemical Toxicology. 2011;49(6):1224-1228.
26. . International journal of pharmaceutical sciences and research. 2012;2012(10).
27. Sestili P, Martinelli C, Ricci D, Fraternale D, Bucchini A, Giamperi L, et al. Cytoprotective effect of preparations from various parts of Punica granatum L. fruits in oxidatively injured mammalian cells in comparison with their antioxidant capacity in cell free systems. Pharmacol Res. 2007;56(1):18-26.
28. Fatima F, Siddiqui S, Khan WA. Nanoparticles as Novel Emerging Therapeutic Antibacterial Agents in the Antibiotics Resistant Era. Biol Trace Elem Res. 2020;199(7):2552-2564.
29. Kim I, Viswanathan K, Kasi G, Thanakkasaranee S, Sadeghi K, Seo J. ZnO Nanostructures in Active Antibacterial Food Packaging: Preparation Methods, Antimicrobial Mechanisms, Safety Issues, Future Prospects, and Challenges. Food Rev Int. 2020;38(4):537-565.
30. An Overview of the Clinical and Laboratory Standards Institute (CLSI) and Its Impact on Antimicrobial Susceptibility Tests. Antimicrobial Susceptibility Testing Protocols: CRC Press; 2007. p. 15-20.
31. Wilson ME, Mizer HE, Morello JA. Microbiology in Patient Care. AJN, American Journal of Nursing. 1980;80(3):532-536.
32. Singh M, Lee KE, Vinayagam R, Kang SG. Antioxidant and Antibacterial Profiling of Pomegranate-pericarp Extract Functionalized-zinc Oxide Nanocomposite. Biotechnology and Bioprocess Engineering. 2021;26(5):728-737.
33. Verbič A, Šala M, Jerman I, Gorjanc M. Novel Green In Situ Synthesis of ZnO Nanoparticles on Cotton Using Pomegranate Peel Extract. Materials. 2021;14(16):4472.
34. Debanath MK, Karmakar S. Study of blueshift of optical band gap in zinc oxide (ZnO) nanoparticles prepared by low-temperature wet chemical method. Mater Lett. 2013;111:116-119.
35. Li F, Li P, Zhang H. Preparation and Research of a High-Performance ZnO/SnO_2 Humidity Sensor. Sensors. 2021;22(1):293.
36. Wang Y, Yang X, Lou J, Huang Y, Peng J, Li Y, et al. Enhance ZnO Photocatalytic Performance via Radiation Modified g-C3N4. Molecules. 2022;27(23):8476.
37. Guo L, Ji YL, Xu H, Simon P, Wu Z. Regularly Shaped, Single-Crystalline ZnO Nanorods with Wurtzite Structure. Journal of the American Chemical Society. 2002;124(50):14864-14865.
38. Khan MI, Kathait GS, Islam MU, Mir FA, Shah AA, Ahmed I, et al. Study of Structural, Crystallite Size, and Optical Properties of Sol–Gel Synthesized Zinc Oxide Nanoparticles Using XRD and UV-Visible Techniques. Physics of the Solid State. 2025;67(2):128-139.
39. Jayappa MD, Ramaiah CK, Kumar MAP, Suresh D, Prabhu A, Devasya RP, et al. Green synthesis of zinc oxide nanoparticles from the leaf, stem and in vitro grown callus of Mussaenda frondosa L.: characterization and their applications. Applied Nanoscience. 2020;10(8):3057-3074.
40. Shaban AS, Owda ME, Basuoni MM, Mousa MA, Radwan AA, Saleh AK. Punica granatum peel extract mediated green synthesis of zinc oxide nanoparticles: structure and evaluation of their biological applications. Biomass Conversion and Biorefinery. 2022;14(11):12265-12281.
41. Mahmoud EAM, Kishk YFM, Khalifa I, Abdel Fattah AFA, Mahdy SM. Boosting antioxidative polyphenols extraction efficiency via nano sized pomegranate peel particles. Sci Rep. 2025;15(1).
42. Ben-Ali S, Akermi A, Mabrouk M, Ouederni A. Optimization of extraction process and chemical characterization of pomegranate peel extract. Chemical Papers. 2018;72(8):2087-2100.
43. Babayevska N, Przysiecka Ł, Iatsunskyi I, Nowaczyk G, Jarek M, Janiszewska E, et al. ZnO size and shape effect on antibacterial activity and cytotoxicity profile. Sci Rep. 2022;12(1).
44. Zubair N, Al-Oqaili RMS, Yousaf MJ, Siddique A, Awwad FA, Ismail EAA, et al. Morphology dependent antibacterial activity of zinc oxide nanoparticles against clinically relevant bacteria. Sci Rep. 2025;15(1).
45. Premanathan M, Karthikeyan K, Jeyasubramanian K, Manivannan G. Selective toxicity of ZnO nanoparticles toward Gram-positive bacteria and cancer cells by apoptosis through lipid peroxidation. Nanomed Nanotechnol Biol Med. 2011;7(2):184-192.
46. Patwekar M. Peer Review #1 of "Green synthesis of silver nanoparticles using Ocimum sanctum Linn. and its antibacterial activity against multidrug resistant Acinetobacter baumannii (v0.2)". PeerJ; 2023.
47. Rizwan M, Singh M, Mitra CK, Morve RK. Ecofriendly Application of Nanomaterials: Nanobioremediation. Journal of Nanoparticles. 2014;2014:1-7.
48. Zinc Oxide Nanoparticles (ZnO-NPs). Encyclopedia of Nanotechnology: Springer Netherlands; 2016. p. 4407-4407.